Use of ab Initio Calculations toward the Rational Design of Room Temperature Ionic Liquids

Elizabeth A. Turner, Cory C. Pye,* and Robert D. Singer*

Department of Chemistry, Saint Mary's University, Halifax, Nova Scotia, Canada B3H 3C3

Received: July 22, 2002; In Final Form: January 31, 2003

Ionic liquids are gaining substantial interest as alternative reaction media. Despite the overwhelming amount of evidence suggesting a relationship between their structure and melting point, there still remains the problem of selectively choosing a particular ionic pair that will produce a liquid at room temperature. Ionic liquids based on 1-alkyl-3-methylimidazolium halides have been investigated using ab initio calculations utilizing Gaussian 98 and the 6-31G* and 6-31+G* basis sets. The calculated interaction energy was found to increase in magnitude with decreasing alkyl chain length at the Hartree−Fock level, although no trend was found to exist with increasing anionic radius. Correlations between melting point and interaction energy were investigated. Linear trends were found to exist in the 1-*n*-butyl-3-methylimidazolium (Bmim) halide series as well as the 1-alkyl-3-methylimidazolium iodide series.

Introduction

Ionic liquids are a class of novel compounds composed exclusively of organic cations and inorganic anions. Unlike ionic solids, in which the ions are relatively small and thus can pack closely to each other, the bulkiness of both the cation and anion prevents such packing, thereby lowering the lattice energy. Consequently, ionic liquids have been classified as ionic compounds that have melting points at temperatures of 100 °C or lower. In fact, many are liquid at or below room temperature, having melting points as low as −96 °C.[1]

The appeal of ionic liquids extends beyond their low melting point. Ionic liquids have negligible vapor pressure and thus are nonvolatile and nonflammable.[2] This nonvolatile nature suggests that ionic liquids might potentially be green alternatives to the use of conventional volatile organic solvents. Ionic liquids are also highly solvating, yet noncoordinating, with a large liquid range.[3] Physical properties such as melting point, density, viscosity, and hydrophobicity can be adjusted through variation of both the cation and anion to tailor a particular ionic liquid for a given end use; hence ionic liquids have been referred to as "designer solvents".[4] It is such tunable physical properties that have led to the application of ionic liquids as solvents for synthesis[5,6] and catalysis[7,8] and as alternative media for extractions[9,10] and purifications.[11,12]

In recent years, the number of possible cation and anion combinations has increased significantly such that researchers believe 1 trillion room temperature ionic liquids could possibly exist.[13] The synthetic problem of being able to rationally design ambient temperature ionic liquids through variation of the anion and cation still remains to be thoroughly investigated, despite attempts to correlate structure with melting point. It is thus essential to develop a systematic method of selectively choosing a given ionic pair, to be used as a predictive tool in the rational design of new ionic liquids.

Currently there has been substantial growth in the number of theoretical investigations pertaining to ionic liquids, whereby scientists are attempting to predict many of the physical properties that characterize ionic liquids. Some of these studies have compared calculated versus experimental values for several physical properties using Monte Carlo simulations[14] whereas others have relied on molecular descriptors generated by a CODESSA program to correlate the melting point of ionic liquids (pyridinium, imidazolium, and benzimidazolium bromides) with structure.[15,16] Ab initio calculations have also been used but to a lesser extent where only the anion of the ionic liquid has been treated and used to predict vibrational frequencies.[17] It is thought that an ab initio investigation of imidazolium based ionic liquids could be used in the calculation of interaction energy between cation and anion, which could potentially be used in a correlation with melting point.

Described herein is an ab initio investigation of 1-alkyl-3-methylimidazolium halides in which the interaction energies were determined for those structures with lowest calculated energies and which closely correspond to known X-ray crystal structures. A search for a correlation between measured melting points and calculated interaction energies was carried out.

Results and Discussion

Computational Analysis. Ionic liquids have not previously been analyzed using ab initio calculations with the intent of developing a correlation with melting points. It is thus necessary to develop a logical and systematic approach to their study. A stepping stone approach was used, starting with the imidazolium ring and adding successive carbon units until the desired cation was constructed. A halide counterion was then added to the cation and re-optimized in the manner described in detail below.

Study of Imidazolium-Based Cations. The imidazolium (Im) ring is present in all structures investigated. The aromatic C_{2v} Im cation (Figure 1) was found to be a planar minimum on the potential energy surface (PES). A methyl group was then added to one of the nitrogen atoms to give methylimidazolium (Mim) in one of two possible orientations of C_s symmetry. Structure Mim 2 has one imaginary frequency (methyl rotation, ∼100i cm^{-1}) of irreducible representation A″ and is higher in energy than the stable Mim 1 structure (Table 1). Given this result, a second methyl group bound to the other nitrogen atom should

* Corresponding author. E-mail: Robert.Singer@stmarys.ca.

10.1021/jp021694w CCC: $25.00
Published on Web 03/11/2003

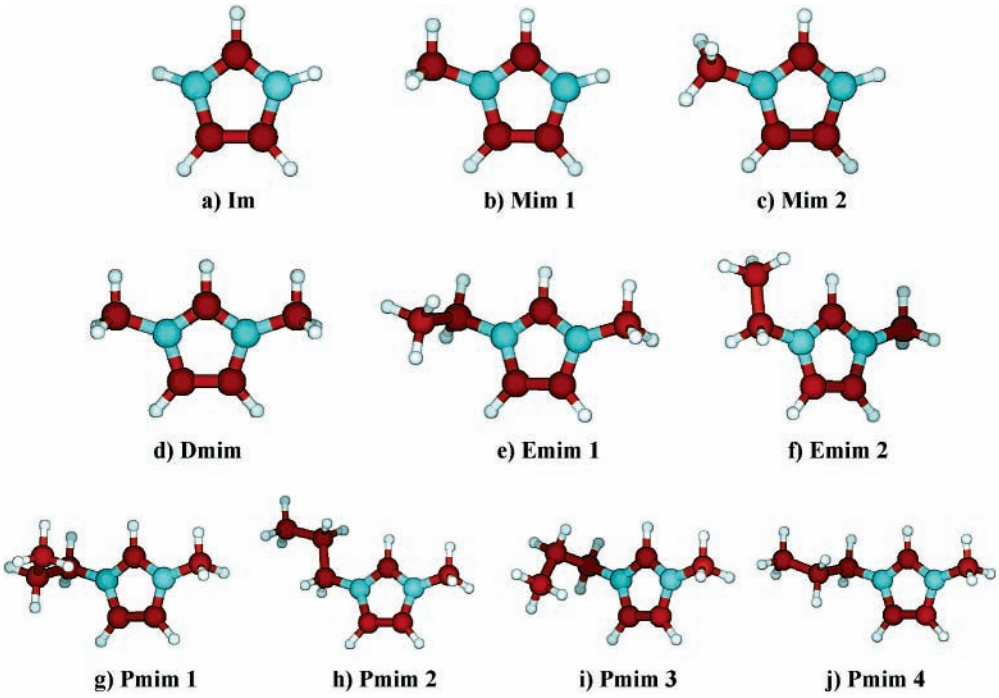

Figure 1. Optimized structures from the investigation of imidazolium, 3-methylimidazolium, and 1-alkyl-3-methylimidazolium based analogues, where R (alkyl) = methyl, ethyl, and *n*-propyl.

TABLE 1: Difference in Energy between the Most Stable and Less Stable Structures of Imidazolium and 1-Alkyl-3-methylimidazolium Based Ionic Liquids, Where R (Alkyl) = Methyl, Ethyl, *n*-Propyl, and *n*-Butyl

	energy difference (kJ mol^{-1})	
level	Mim 2−1	Emim 2−1
HF/STO-3G	1.50	4.01
HF/3-21G	2.28	2.90
HF/6-31G*	2.94	3.25
HF/6-31+G*	3.03	3.24
MP2/6-31G*	2.08	3.27
MP2/6-31+G*	1.70	4.11

	energy difference (kJ mol^{-1})			
level	Pmim 2−1	Pmim 3−1	Pmim 4−1	Bmim 2−1
HF/STO-3G	2.88	0.98	−1.64	3.76
HF/3-21G	3.40	1.96	−0.14	2.73
HF/6-31G*	2.81	2.23	−1.07	3.93
HF/6-31+G*	2.86	2.48	−1.10	4.17
MP2/6-31G*	5.85	1.66	1.94	1.42
MP2/6-31+G*	8.08	1.92	2.92	1.73

	energy difference (kJ mol^{-1})			
level	Bmim 3−1	Bmim 4−1	Bmim 5−1	Bmim 6−1
HF/STO-3G	9.34	1.84	−1.72	1.88
HF/3-21G	11.21	2.78	0.03	2.85
HF/6-31G*	11.02	2.70	−1.13	2.82
HF/6-31+G*	11.02	2.74	−1.17	2.87
MP2/6-31G*	6.98	4.64	2.39	4.69
MP2/6-31+G*	5.48	6.00	3.78	6.01

	energy difference (kJ mol^{-1})			
level	Bmim 7−1	Bmim 8−1	Bmim 9−1	Bmim 10−1
HF/STO-3G	4.73	1.02	10.21	2.68
HF/3-21G	4.57	1.96	12.66	3.14
HF/6-31G*	6.14	2.24	13.18	2.41
HF/6-31+G*	6.62	2.52	13.34	2.48
MP2/6-31G*	3.16	1.66	8.43	5.92
MP2/6-31+G*	3.79	1.91	7.13	8.71

have the same orientation as in Mim 1, and, indeed, a stable C_{2v} structure for dimethylimidazolium (Dmim) was found.

The next step involved progressively adding methylene units to one of the methyl groups to form ethylmethyl- (Emim), *n*-propylmethyl- (Pmim), and *n*-butylmethylimidazolium (Bmim). All possible rotamers were optimized. For Emim, there are two possibilities, a planar C_s (Emim 2) and the more stable nonplanar C_1 structure (Emim 1). The methyl(ene) orientation adjacent to the nitrogen is retained. The smallest frequencies, corresponding to methylene rotation, are always less than 50 cm^{-1}. The C_1 structure (at all levels) and the C_s structure (at the HF levels only) were found to produce no imaginary frequencies. However, the C_s structure, at the MP2 levels, gave one small imaginary frequency (<40i cm^{-1}) of irreducible representation A″ corresponding to methylene rotation. The small magnitude suggests that this may be an artifact, so a relaxed PES scan was performed. This indicated that the region was so flat that no definitive statement could be made (a 10° change in the dihedral decreased the energy by 0.007 kJ/mol).

The three staggered conformations of the terminal methyl of a propyl substituent, taken with the results above, give rise to a total of six possible conformations of Pmim. A C_s structure can be derived from Emim 2 (Pmim 2), which also has an imaginary frequency at the MP2 levels. The other initial structures derived from Emim 2 had severe steric interactions between the terminal methyl group and hydrogen two of the imidazolium ring and coalesced into Pmim 1, which was the most stable conformation (Table 1) at the MP2 levels. However, Pmim 4 was most stable at the HF levels.

The three staggered conformations of the terminal methyl of a butyl substituent, taken with the results above, give rise to a total of twelve possible conformations of Bmim. A C_s structure can be derived from Pmim 2 (Bmim 10, Figure 2), which also has an imaginary frequency at the MP2 levels. The most stable structure is Bmim 1 (Table 1). Two of the structures, derived from Pmim 2, coalesced into other structures. Bmim 1−3 are derived from Pmim 1, Bmim 4−6 are derived from Pmim 4, and Bmim 7−9 are derived from Pmim 3. We note that within the three sets derived from the same propyl conformation, the

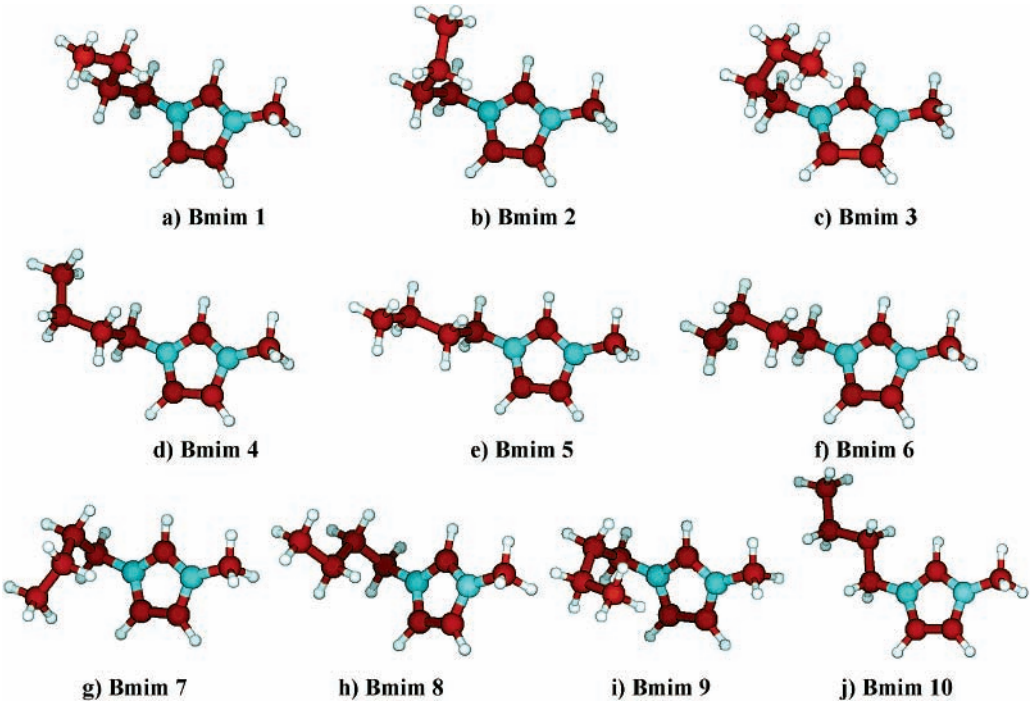

Figure 2. All optimized structures from the investigation of 1-*n*-butyl-3-methylimidazolium.

zigzag conformations of the butyl group are the most stable (Bmim 1, 5, 8). The two conformations in which the methyl group is positioned over (and sterically interacting with) the ring are the least stable (Bmim 3, 9).

1-Ethyl-3-methylimidazolium Fluoride. 1-Ethyl-3-methylimidazolium fluoride was not prepared synthetically. Nevertheless it was chosen as the initial system for investigation, as fluoride has fewer electrons than the other halides and thus simpler to calculate at a given level. The optimized geometry and orientation (Z-matrix) for the Emim 1 cation was constrained (origin C2, C2−H2 defines *z*-axis, C2−H2−N1 defines the *xz* plane) and an imaginary gridded box (1 Å spacing) was constructed surrounding the cation, spanning approximately 2 Å away from the closest atom on each face. The atomic *x* and *z* coordinates had ranges of (−3.02 to +4.13) and (−2.94 to +1.08), respectively. For the six box faces generated, the fluoride ion (as defined by Cartesian coordinates) was allowed to move to each position of the grid where a HF/STO-3G energy was calculated. The six scans thus corresponded to fluorine positions (−5.0 to +6.0, +2.0, −5.0 to +3.0), (−5.0 to +6.0, −2.0, −5.0 to +3.0), (−5.0 to +6.0, −2.0−2.0, −5.0), (−5.0 to +6.0, −2.0 to +2.0, +3.0), (−5.0, −2.0 to +2.0,−5 to +6.0), and (+6.0, −2.0 to +2.0, −5.0 to +6.0). The results of these rigid PES scans are summarized as both three-dimensional and contour plots (Figure 3). This gives us a coarse estimate as to possible positions of fluoride. From these plots, sixteen regions of local minima were determined for the six surfaces as labeled in Figure 3. The collision of the fluoride with the ethyl group is clearly seen as a maximum in Figure 3a. The scans were followed by partial fluoride-only optimizations (HF/STO-3G) starting with each of the potential minima. The structures associated with minima 13, 14, and 15 were found to coalesce with those calculated for minima 8, 3, and 5, respectively. These redundant structures resulted from faces sharing a common edge of the box and were removed from further study.

The remaining structures were then fully optimized. In all cases except for minimum 5 (Emim F (5), Figure 4), the structures converged at HF/STO-3G. Further attempts to optimize this minimum, characterized as the E_2 product of attack of the base F^- on $Emim^+$, (ethene, leaving group methylimidazole and conjugate acid hydrogen fluoride), resulted in further separation, and therefore the structure was removed from further study.

HF/6-31G* analysis revealed that the remaining structures could be divided into two classes. In the case of minima 3, 8, 9, 11, 12, and 16 the structure was found to have removed a hydrogen from one of the ring carbons, forming hydrogen fluoride (Figure 4), whereas the structures for minima 1, 2, 4, 6, 7, and 10 had covalently bound fluorine to one of the ring carbons (Figure 5). It is interesting that carbene-like species (Figure 4) were predicted by our calculations. The most stable of these (Figure 4d) possesses a carbene carbon flanked by two heteroatoms bearing lone pairs of electrons. The stability of these species may help explain the inability to prepare dialkylimidazolium fluoride salts from *N*-methylimidazole and an alkyl fluoride. As it was felt that hydrogen fluoride would remain at the higher levels of theory, these structures were removed from further investigation and only those in which fluorine was covalently bound to carbon were studied at higher levels of theory.

No structure yet obtained has ionic character, and all structures were found to have a covalently bound fluorine at the higher HF/6-31+G* and MP2/6-31G* levels. The structures represented by minima 1, 2, 6, and 7, however, were found to dissociate at MP2/6-31+G*, finally producing the ionic Emim fluoride (Figure 5b,e). The remaining two structures in the analysis (represented by minima 4 and 10) were found to maintain the same covalent configuration at MP2/6-31+G*.

The structures for minimum 4 and 10 were found (Table 2) to be the most favored isomers of 1-ethyl-3-methylimidazolium fluoride (1-ethyl-2-fluoro-3-methyl-2,3-dihydro-1*H*-imidazole). These two structures are the only possible forms in which stable Lewis structures can be drawn. The other covalent structures, including those containing discrete HF units, can only be written using charge-separated or carbene Lewis structures. Thus for fluoride, covalent bonding is preferred over the desired ionic

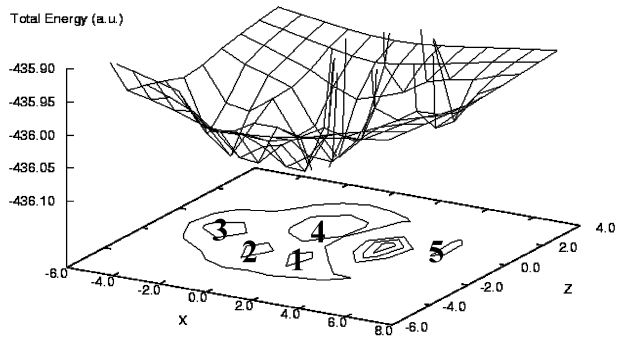

a) y = 2.0 Å

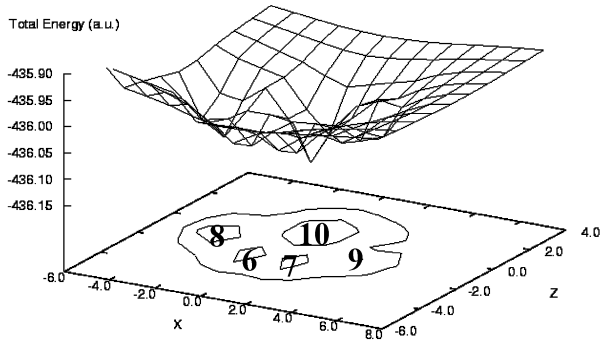

b) y = -2.0 Å

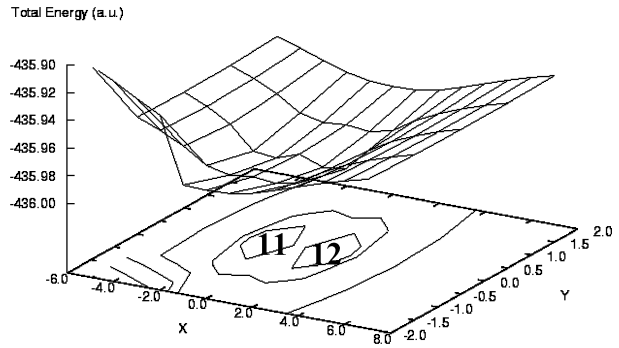

c) z = -5.0 Å

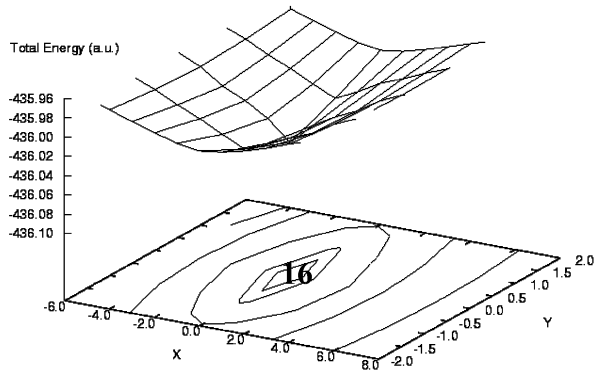

d) z = 3.0 Å

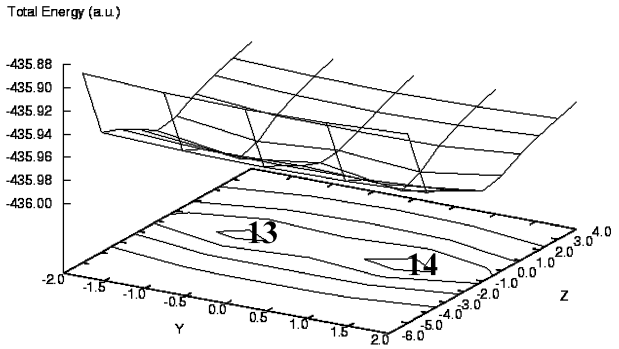

e) x = -5.0 Å

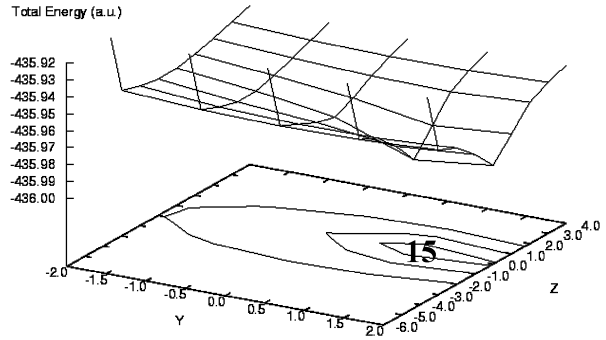

f) x = 6.0 Å

Figure 3. Potential energy surface scan plots for 1-ethyl-3-methylimidazolium fluoride.

form. Ab initio theory thus provides insight as to why fluoride is not selected as an anion when designing ionic liquids, as the anion is likely to bond covalently to the ring.

1-Ethyl-3-methylimidazolium Halides. The study of the 1-ethyl-3-methylimidazolium chloride, bromide, and iodide-based ionic liquids utilized the HF/STO-3G Emim fluoride parameters for each of the four fully studied fluoride systems, with the fluoride replaced by the appropriate halogen in the Z-matrix. The study of Emim chloride gave two different ionic structures (Figure 6), where the chloride was positioned in the plane of the ring. Emim Cl 1 was the more stable of the two (Table 2). The position of chloride in the stable structure was found to agree with the literature crystal structure,[21] whereby the chloride, found in the plane of the ring, is associated with the hydrogen of carbon two of the ring, positioned closer to the methyl substituent as opposed to the ethyl substituent. It is surprising, yet encouraging, that these gas phase calculations give the same structure as the solid phase crystal structure.

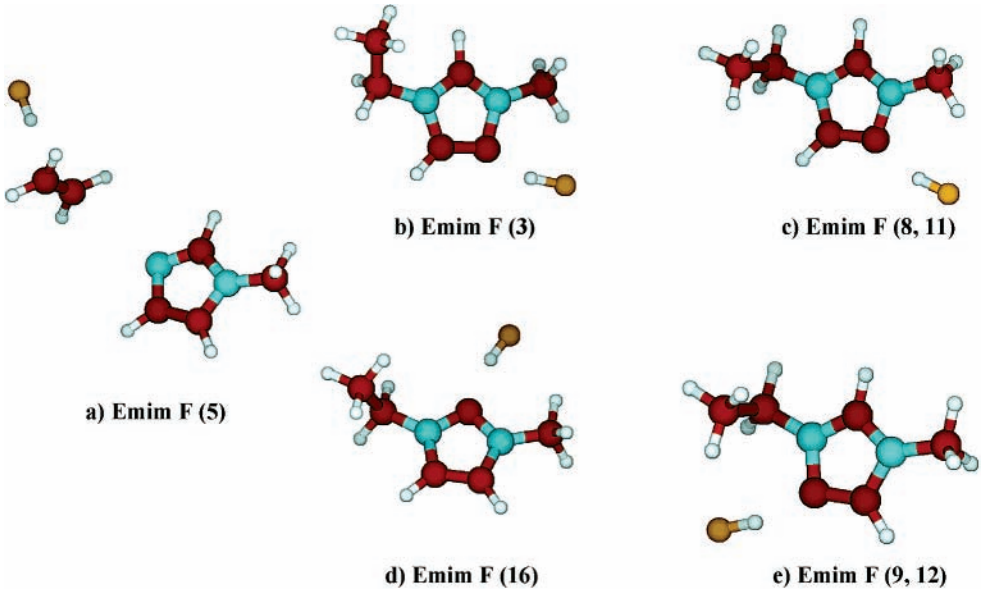

Figure 4. Deprotonated structures from the study of 1-ethyl-3-methylimidazolium fluoride. (a) Structure producing methylimidazole, ethene, and hydrogen fluoride. (b)−(e) Structures optimized at HF/6-31G* that produced hydrogen fluoride.

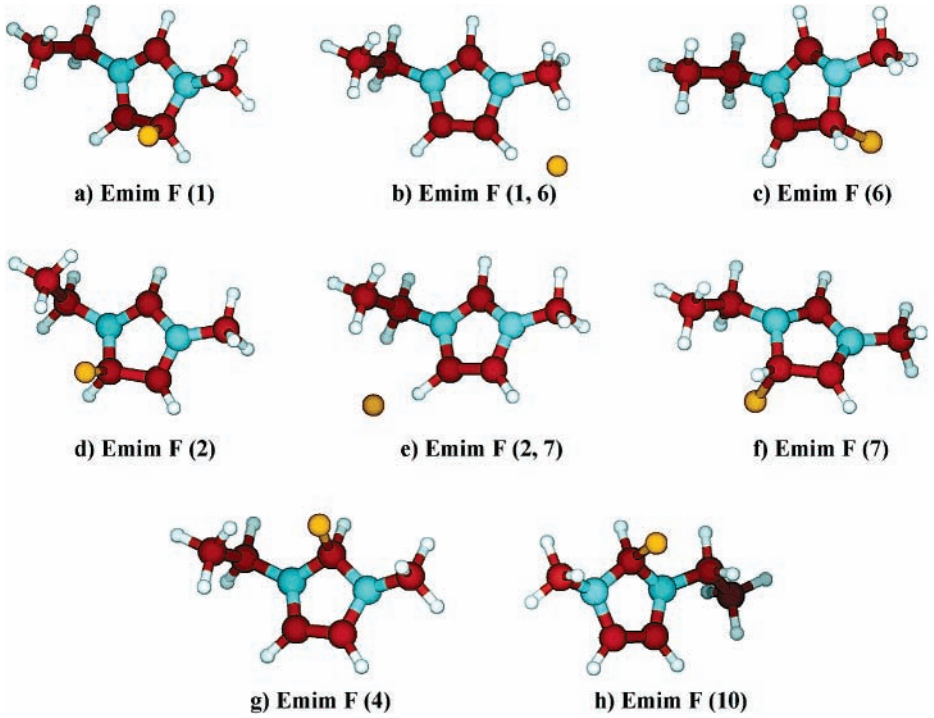

Figure 5. (a), (c), (d), (f) MP2/6-31G* structures from the study of 1-ethyl-3-methylimidazolium fluoride. (b), (e), (g), (h) MP2/6-31+G* optimized structures from the study of 1-ethyl-3-methylimidazolium fluoride.

Unlike the fluoride, the chloride dissociated at the relatively inexpensive HF/3-21G level and remained dissociated.

The Emim bromide study gave three different ionic structures (Figure 6). Emim Br 1 was found to be the most stable structure (Table 2). Emim Br 3 coalesced with that of Emim Br 1 at the MP2 levels. Unlike the chloride system, where the chloride was found in the plane of the ring, the bromide of the most stable structure was found to be above the ring plane.

There was a significant disagreement with respect to the position of the bromide in the calculated system and in the crystal structure.[22] The crystal structure indicates that the bromide resides in the ring plane, located in the same relative position as the chloride. Comparison of the calculated (0.297 nm) versus experimental (0.278 nm) hydrogen bond distance between bromide and hydrogen two of the ring, however, suggests that the anion has approximately the same distance from the cation but differs in spatial orientation. This nonplanar anion geometry is discussed later.

The Emim iodide study gave two different ionic structures (Figure 6), wherein the anion was within the plane of the ring. Emim I 1 was the most stable structure agreeing, with respect to the position of the anion, with the crystal structure.[23] The hydrogen bond distance in the calculated structure (0.285 nm) was found to agree with the literature (0.293 nm).

TABLE 2: Difference in Energy between the Most Stable and Less Stable Structures of 1-Ethyl-3-methylimidazolium Halides, Where X (Halide) = Fluoride, Chloride, Bromide, and Iodide

	energy difference (kJ mol^{-1})		
level	Emim F 1−4	Emim F 2−4	Emim F 3−4
HF/STO-3G	249.52	250.72	411.70
HF/3-21G	183.66	175.61	
HF/6-31G*	161.99	162.50	
HF/6-31+G*	146.25	148.62	
MP2/6-31G*	102.54	100.51	
MP2/6-31+G*	35.06	33.80	

	energy difference (kJ mol^{-1})		
level	Emim F 6−4	Emim F 7−4	Emim F 8−4
HF/STO-3G	246.90	252.27	412.20
HF/3-21G	182.90	183.71	111.63
HF/6-31G*	161.06	163.11	103.27
HF/6-31+G*	147.40	147.20	
MP2/6-31G*	102.57	104.83	
MP2/6-31+G*	35.06	33.80	

	energy difference (kJ mol^{-1})		
level	Emim F 9−4	Emim F 10−4	Emim F 11−4
HF/STO-3G	417.10	−0.43	317.36
HF/3-21G	111.98	8.15	111.62
HF/6-31G*	99.16	−1.32	103.27
HF/6-31+G*		−2.79	
MP2/6-31G*		2.40	
MP2/6-31+G*		1.09	

	energy difference (kJ mol^{-1})		
level	Emim F 12−4	Emim F 16−4	Emim Cl 2−1
HF/STO-3G	314.71	170.75	142.49
HF/3-21G	110.24	22.18	41.24
HF/6-31G*	99.16	14.54	41.21
HF/6-31+G*			41.32
MP2/6-31G*			34.63
MP2/6-31+G*			31.82

	energy difference (kJ mol^{-1})		
level	Emim Br 2−1	Emim Br 3−1	Emim I 2−1
HF/STO-3G	202.28	−7.61	143.97
HF/3-21G	44.87	2.76	38.99
HF/6-31G*	43.98	4.17	37.66
HF/6-31+G*	43.37	5.39	38.49
MP2/6-31G*	40.11	0.0026	29.94
MP2/6-31+G*	49.25	0.00026	31.42

As stated, the anion position of Emim bromide was considerably different than that of Emim chloride and iodide. The bromide systems were re-optimized, in which optimized chloride and iodide parameters were applied to the bromide system, to determine whether Emim bromide could be optimized such that the bromide would remain in the ring plane and vice versa. The systems were analyzed at all levels of theory, but in each case, the new systems were found to coalesce in energy to their previously determined stable structures. By repeating the procedure just for the MP2/6-31+G* level, we were able to obtain additional planar geometries (Figure 6h). This suggests that the developed methodology to find minima has some shortcomings. As a check, we re-optimized the chloride and iodide systems, using the nonplanar bromide parameters and obtained nonplanar geometries (Figure 6d,k). The nonplanar structures were more stable than the planar structures at the highest level.

The minimum-energy nonplanar structure of chloride might appear as a local minimum if a PES scan, similar to that carried out for Emim fluoride, was performed. A similar gridded box was constructed around the Emim cation, spanning approximately 2.5 Å from the closest atom on each face. The results of these HF/STO-3G rigid PES scans are summarized as both three-dimensional and contour plots (Figure 7). In total, seventeen possible minima were located from the six surfaces examined. Comparison of the fluoride and chloride PES scans indicated that the results were essentially the same. In many cases what appeared as two local minima in the Emim fluoride scan only appeared as one large localized minimum in the Emim chloride scan.

Only one new minimum resulted from this (Emim Cl 4) and was higher in energy than that of the nonplanar geometry. The anion was localized near C5 of the imidazolium ring. In the original study, one of the structures initially had chlorine bound to C5, which immediately dissociated during optimization at the HF/STO-3G level; however, instead of the ion remaining around the C5 position, it migrated across the plane of the ring and optimized to the most stable Emim Cl 1 structure.

There are two types of minima found in these systems. One type has the halogen positioned over the ring, whereas the other type has the halogen positioned in the plane of the ring interacting with (at least) two hydrogens. Generally, the first type is energetically preferred. Of the structures of the second type, those halogens positioned to interact with H−C(2) generally have the lowest energy. This makes sense as this hydrogen is the most acidic (the carbene resulting from deprotonation is stabilized by two adjacent nitrogens).

1-Alkyl-3-methylimidazolium Halides. The propyl and butylmethylimidazolium halides were investigated in the same manner as the ethyl analogue, the results of which were essentially the same. The initial systems were generated using the optimized parameters from the corresponding most stable cation system previously studied.

In the case of the chloride based ionic liquids (Pmim Cl 1; Figure 8, Bmim Cl 1; Figure 9), the most stable structure (Tables 3 and 4) had the anion positioned in the plane of the heterocyclic ring, as was observed in the ethyl study. The most stable bromide based ionic liquids (Pmim Br 1, Bmim Br 1) were again found to position the anion above the plane of the ring.

The iodide based ionic liquids deviated slightly from the result observed in the ethyl study. In both cases the iodide was found to move from the plane of the heterocyclic ring and orient over the heterocyclic ring. The movement was much more significant in the case of Pmim iodide. It is noteworthy that this stable structure is the lowest energy structure only at the highest level of theory (Table 3).

Interaction Energy. The interaction energy is defined as the difference between the energy of the ionic system (E_{AX}) and the sum of the energies of the purely cationic (E_{A^+}) and anionic (E_{X^-}) species.

$$E\ (\text{kJ/mol}) = 2625.5[E_{AX}\ (\text{au}) - E_{A^+}\ (\text{au}) + E_{X^-}\ (\text{au})]$$

Within an alkyl chain series, there was no apparent trend found between interaction energy and anion identity (Table 5). Upon examining the transition from chloride to iodide a nonlinear energy change at both HF/6-31+G* and MP2/6-31+G* resulted. Presuming that ion bulkiness is the predominant factor determining the magnitude of electrostatic attraction, it should thus be expected that the interaction between cation and anion would decrease upon increasing anionic radius. The chloride ion should then be expected to pack closer to a given cation

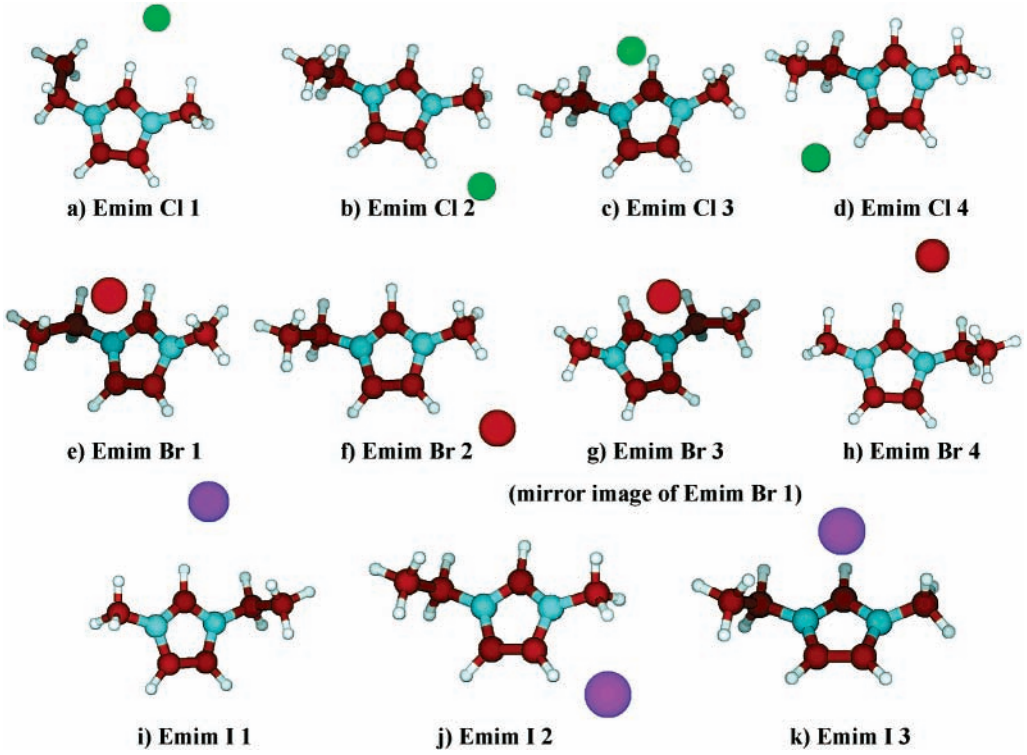

Figure 6. Optimized structures from the study of 1-ethyl-3-methylimidazolium halides: (a)−(c) chloride based ionic liquids; (d)−(g) bromide based ionic liquids; (h)− (j) iodide based ionic liquids.

than bromide or iodide and hence have the greatest interaction whereas iodide should have the smallest. In the case of bromide however, there was a significant increase in interaction in the transition from chloride to bromide, thus eliminating a linear trend between the three halides. The deviation from linearity is likely the result of the different geometry observed in the case of bromide.

For a given anionic series the magnitude of interaction decreased as a function of increasing alkyl chain length only at HF/6-31+G*. The trend ceases to exist at the MP2/6-31+G* level of theory, especially in the case of bromide and iodide where linearity was disrupted, whereas this same linear effect was reversed in the case of chloride; the longer the alkyl chain length, the greater the interaction.

Correlation of Interaction Energy and Melting Point. Gross trends relating interaction energy and melting point were found within the chloride, bromide, and iodide series (Figure 10). Where possible, the structure corresponding to the known X-ray data was taken. For the bromides, the structures were different, which would introduce some scatter in the results. The analysis of the iodide series revealed a "linear" trend, in which the melting points of the iodide based ionic liquids were found to decrease with increasing chain length, and this was associated with a decrease in the magnitude of interaction energy. The difference between successive melting points, however, was much greater than the difference between successive energies.

In the case of the chloride and bromide based ionic liquids, the melting point of the Pmim analogue was significantly lower than that of the Emim and Bmim analogues, although the interaction was found to increase in magnitude with increasing alkyl chain length. The resulting correlation could be the beginning of a saw-tooth pattern, a trend previously reported for the melting point behavior of unbranched alkanes.[24] The saw-tooth melting point behavior is often observed within a series of alkanes whereby those with an even number of carbons lie on a separate and higher curve than those with an odd number of carbons. This behavior reflects the more effective packing of the even-carbon alkanes in the crystalline state. It is possible that this packing effect also occurs for the chloride and bromide based 1-alkyl-3-methylimidazolium halides. Difficulties with the purification of the Pmim series and the resulting melting points make it difficult to establish this with certainty.

A trend was also found to exist in the Bmim halide series, where the melting point increase between Bmim chloride and Bmim bromide was associated with an increase in magnitude of the interaction. The melting point was then found to decrease significantly between Bmim bromide and Bmim iodide, and this was associated with a significant decrease in magnitude of the interaction.

Our preliminary investigation of a series of three cations paired with three anions, provides some initial hints as to the relationship between the interaction energy and the melting point. These results suggest that there is more than one factor contributing to the melting point behavior of ionic liquids based on 1-alkyl-3-methylimidazolium halides. It is possible that for certain systems the melting point is governed more strongly by the cation than the anion and vice versa and also a balance between Coulombic attractions of oppositely charged ions and van der Waals repulsions of the alkyl chains on the imidazolium cation. The results suggest that further investigation with other ion pairs should clarify the existence and nature of correlations with the melting temperature of ionic liquids.

Our studies have shown that structures calculated using ab initio methods correlate with those obtained from X-ray crystallographic analysis; however, such computations have proven to be quite "time" expensive. We are endeavoring to refine correlations and improve on our models to overcome the limitations of the computational methods used in our study.

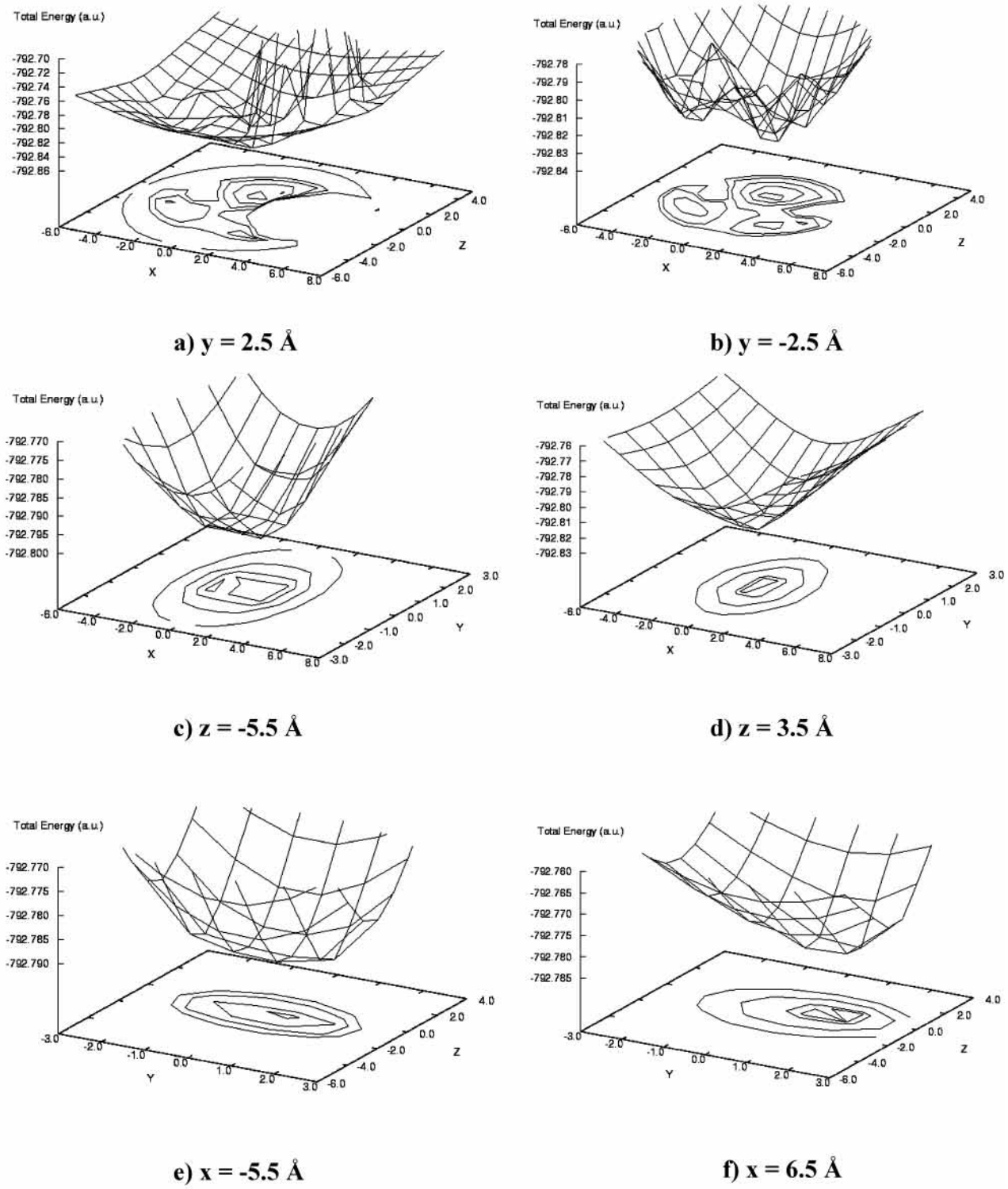

Figure 7. Potential energy surface scan plots for 1-ethyl-3-methylimidazolium chloride.

Experimental Section

Synthesis. Melting points and heats of fusion were obtained using a Mettler FP85 differential scanning calorimetry (DSC) cell in conjunction with a Mettler FP80 central processing unit at 2 °C/min between 50 and 100 °C, on 6−13 mg samples. Prior to preparing the DSC sample, all aluminum sample pans were dried in an oven (110 °C) until a constant weight was obtained. Due to the hygroscopic nature of the compounds synthesized, DSC sample pans were prepared under an inert argon atmosphere in a glovebox. All melting points were performed in triplicate.

^{1}H and ^{13}C NMR spectra were recorded on a Bruker 250 MHz spectrometer using TMS as an internal standard. Infrared spectra were recorded on a Bruker Vector 22 FTIR.

A representative procedure for the synthesis of 1-alkyl-3-methylimidazolium halides is described for 1-*n*-butyl-3-methylimidazolium chloride. 1-Methylimidazole and a large excess of 1-chlorobutane were injected into an oven-dried, vacuum-

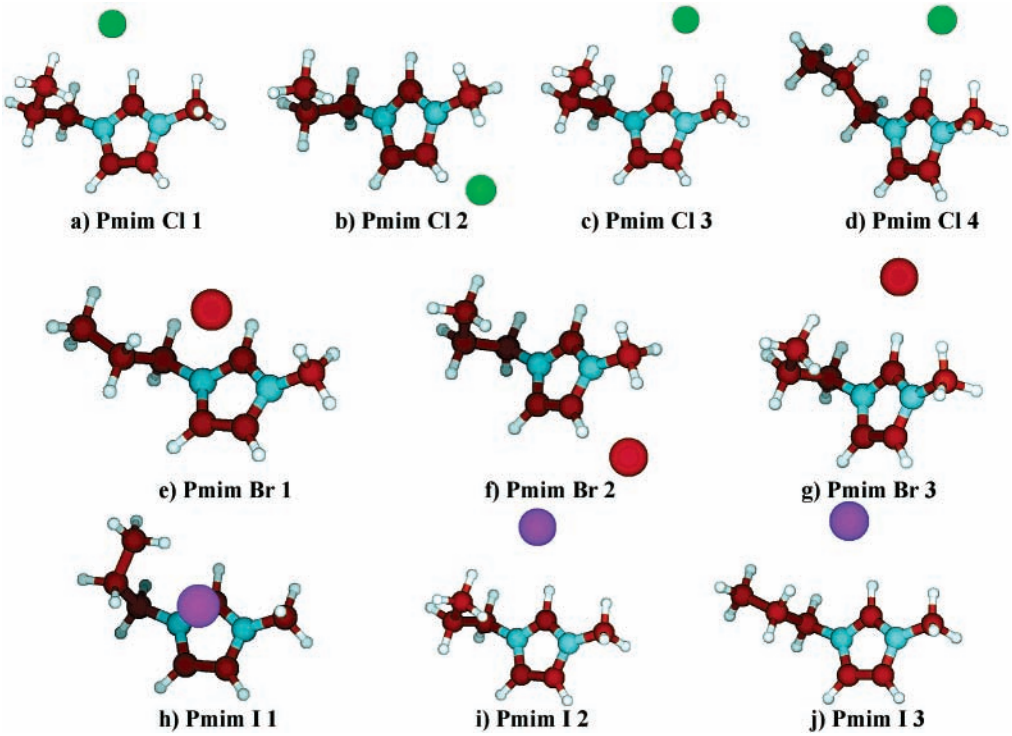

Figure 8. Optimized structures from the study of 1-methyl-3-*n*-propylimidazolium halides: (a)−(d) chloride based ionic liquids; (e)−(g) bromide based ionic liquids; (h)−(j) iodide based ionic liquids.

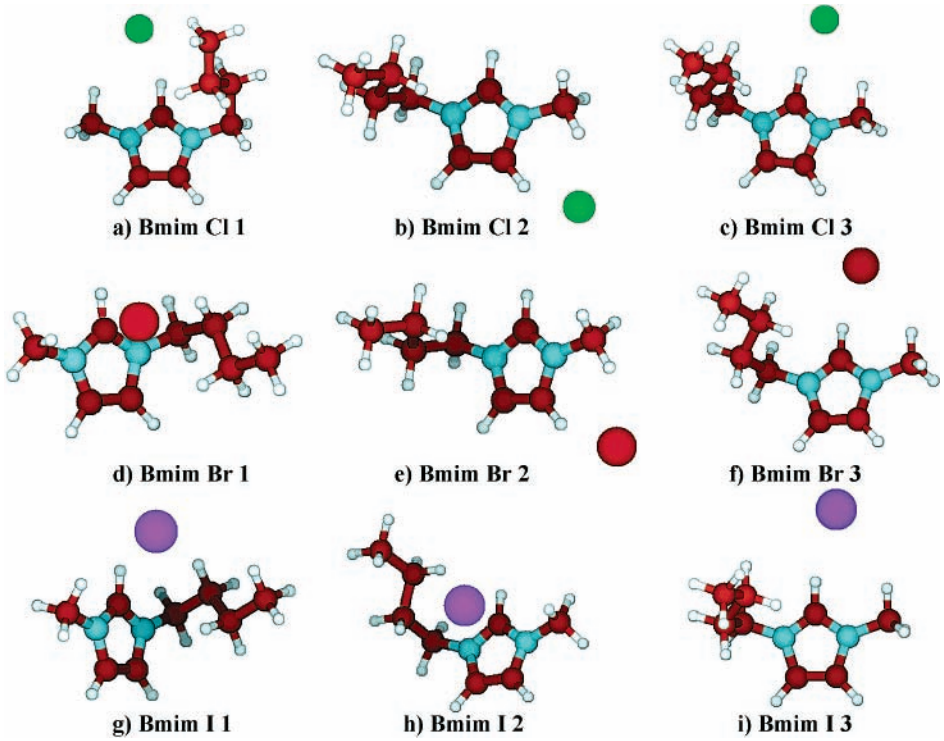

Figure 9. Optimized structures from the study of 1-*n*-butyl-3-methylimidazolium halides: (a)−(c) chloride based ionic liquids; (d)−(f) bromide based ionic liquids; (g)−(i) iodide based ionic liquids.

cooled round-bottomed flask. The flask was fitted with a condenser and allowed to reflux for 24 h. The reaction was completed upon the formation of two phases. The top phase, containing unreacted starting material, was decanted and discarded. The bottom phase was washed three times with ethyl acetate to remove any remaining unreacted reagents. Residual ethyl acetate was removed by heating the bottom phase (80 °C) under vacuum (12 h), which upon cooling, produced a white solid. The product was recrystallized from dry, distilled acetonitrile.

1-*n*-Butyl-3-methylimidazolium Chloride. Yield: 85.62 g, 0.490 mol, 97.6%. Melting point: 68.6 ± 0.2 °C. Heat of fusion: 21.7 ± 0.5 kJ mol^{-1}. ^{1}H NMR (acetone-d_6, δ/ppm relative to TMS): 0.94 (t, $CH_2CH_2CH_2CH_3$, J = 7.4 Hz), 1.37

TABLE 3: Difference in Energy between the Most Stable and Less Stable Structures of 1-Methyl-3-*n*-propyl-imidazolium Halides, Where X = Chloride, Bromide, and Iodide

	energy difference (kJ mol^{-1})		
level	Pmim Cl 2−1	Pmim Cl 3−1	Pmim Cl 4 −1
HF/STO-3G	140.36	12.46	3.73
HF/3-21G	43.76	2.66	3.30
HF/6-31G*	42.16	0.94	0.47
HF/6-31+G*	41.19	0.11	−0.71
MP2/6-31G*	34.91	2.12	3.45
MP2/6-31+G*	34.34	1.44	6.06

	energy difference (kJ mol^{-1})	
level	Pmim Br 2−1	Pmim Br 3−1
HF/STO-3G	196.33	0.73
HF/3-21G	43.65	0.64
HF/6-31G*	44.42	2.48
HF/6-31+G*	43.98	4.43
MP2/6-31G*	37.60	0.46
MP2/6-31+G*	46.44	11.75

	energy difference (kJ mol^{-1})	
level	Pmim I 2−1	Pmim I 3−1
HF/STO-3G	−131.97	−134.07
HF/3-21G	−39.78	−38.27
HF/6-31G*	−37.54	−38.79
HF/6-31+G*	−18.20	−19.63
MP2/6-31G*	−11.18	−9.34
MP2/6-31+G*	2.03	4.18

TABLE 4: Difference in Energy between the Most Stable and Less Stable Structures of 1-*n*-Butyl-3-methyl-imidazolium Halides, Where X = Chloride, Bromide, and Iodide

	energy difference (kJ mol^{-1})	
level	Bmim Cl 2−1	Bmim Cl 3−1
HF/STO-3G	141.02	1.08
HF/3-21G	44.4	3.57
HF/6-31G*	41.6	0.71
HF/6-31+G*	39.6	−1.31
MP2/6-31G*	37.9	5.03
MP2/6-31+G*	35.7	1.71

	energy difference (kJ mol^{-1})	
level	Bmim Br 2−1	Bmim Br 3−1
HF/STO-3G	203.00	1.55
HF/3-21G	48.41	5.73
HF/6-31G*	46.46	4.47
HF/6-31+G*	39.49	−0.73
MP2/6-31G*	48.38	10.41
MP2/6-31+G*	51.91	14.88

	energy difference (kJ mol^{-1})	
level	Bmim I 2−1	Bmim I 3−1
HF/STO-3G	142.49	2.19
HF/3-21G	40.03	1.37
HF/6-31G*	35.50	−1.74
HF/6-31+G*	14.03	−2.40
MP2/6-31G*	9.81	2.24
MP2/6-31+G*	5.46	2.63

(sextet, $CH_2CH_2CH_2CH_3$, J = 7.4 Hz), 1.92 (quint, $CH_2CH_2CH_2CH_3$, J = 7.4 Hz), 4.10 (s, CH_3), 4.45 (t, $CH_2CH_2CH_2CH_3$, J = 7.3 Hz), 7.88 (br s, H_4, H_5), 7.94 (br s, H_4, H_5), 10.862 (s, H_2). ^{13}C NMR (δ/ppm): 12.8, 18.8, 31.6, 35.9, 49.1, 121.7, 123.3, 137.0. IR (thin film on NaCl plates, ν/cm^{-1}): 3140, 3012, 2960, 2935, 2876, 1574, 1468, 1279, 1179, 743, 699, 626.

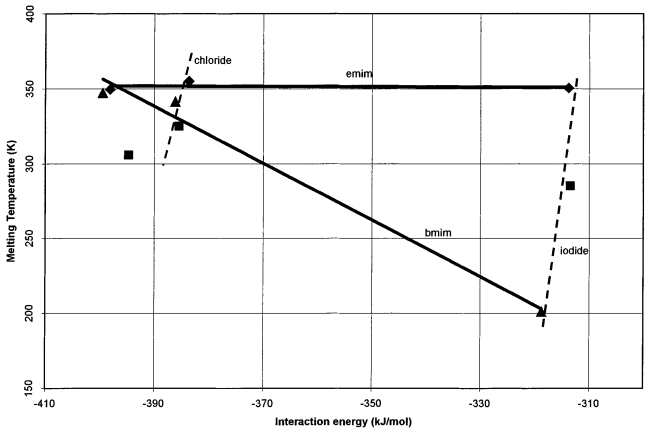

Figure 10. Correlation between melting temperature and interaction energy for ionic liquids studied: (◆) Emim; (■) Pmim; (▲) Bmim.

TABLE 5: Interaction Energies of 1-Alkyl-3-methylimidazolium Halides, Where R = Ethyl, *n*-Propyl, and *n*-Butyl and X = Chloride, Bromide, and Iodide

	interaction energy (kJ mol^{-1})		
level	Emim Cl 1	Emim Br 1	Emim I 1
HF/STO-3G	−555.86	−626.08	−505.17
HF/3-21G	−394.51	−395.74	−341.98
HF/6-31G*	−379.23	−385.84	−320.16
HF/6-31+G*	−361.26	−363.99	−320.55
MP2/6-31G*	−403.78	−409.07	−305.31
MP2/6-31+G*	−383.70	−398.16	−313.84

	interaction energy (kJ mol^{-1})		
level	Pmim Cl 1	Pmim Br 1	Pmim I 1
HF/STO-3G	−550.92	−622.85	−492.59
HF/3-21G	−395.87	−393.37	−341.10
HF/6-31G*	−377.91	−384.04	−318.79
HF/6-31+G*	−359.61	−362.57	−319.29
MP2/6-31G*	−403.00	−370.04	−302.33
MP2/6-31+G*	−385.53	−394.75	−313.49

	interaction energy (kJ mol^{-1})		
level	Bmim Cl 1	Bmim Br 1	Bmim I 1
HF/STO-3G	−550.70	−628.61	−500.21
HF/3-21G	−395.70	−397.27	−341.22
HF/6-31G*	−377.47	−385.06	−315.93
HF/6-31+G*	−357.65	−357.99	−316.60
MP2/6-31G*	−405.00	−415.40	−300.29
MP2/6-31+G*	−386.15	−399.55	−318.78

The remaining ionic liquids were prepared using the same procedure as described for the synthesis of 1-*n*-butyl-3-methylimidazolium chloride, using the corresponding alkyl halide. The iodide based ionic liquids were synthesized in a sufficient volume of dry and distilled tetrahydrofuran. All of the compounds were extremely hygroscopic in nature and those containing an iodide counterion were found to be light sensitive.

1-Ethyl-3-methylimidazolium Bromide. The product was obtained as an off-white solid (23.27 g, 0.124 mol, 99.1%). Melting point: 76.3 ± 0.5 °C. Heat of fusion: 15.7 ± 0.3 kJ mol^{-1}. ^{1}H NMR ($CDCl_3$, δ/ppm relative to TMS): 1.33 (t, CH_2CH_3, J = 7.3 Hz), 3.86 (s, CH_3), 4.16 (quart, CH_2CH_3, J = 7.3 Hz), 7.47 (br s, H_4, H_5), 7.48 (br s, H_4, H_5), 9.96 (s, H_2). ^{13}C NMR (δ/ppm): 15.4, 36.3, 44.9, 121.9, 123.5, 136.3. IR (thin film on NaCl plates, ν/cm^{-1}): 3140, 3073, 3010, 2983, 1574, 1469, 1277, 1175, 724, 698, 622.

1-Ethyl-3-methylimidazolium Iodide. The product was obtained as white solid (93.55 g, 0.393 mol, 97.8%). Melting point: 77.4 ± 0.5 °C. Heat of fusion: 16.5 ± 0.4 kJ mol^{-1}. ^{1}H

NMR (acetone-d_6, δ/ppm relative to TMS): 1.56 (t, CH_2CH_3, $J = 7.3$ Hz), 4.10 (s, CH_3), 4.47 (quart, CH_2CH_3, $J = 7.3$ Hz), 7.88 (br s, H_4, H_5), 7.98 (br s, H_4, H_5), 9.73 (s, H_2). ^{13}C NMR (δ/ppm): 16.1, 37.2, 45.8, 123.2, 124.7, 137.8. IR (thin film on NaCl plates, ν/cm^{-1}): 3140, 3082, 3009, 2951, 2825, 1574, 1467, 1280, 1163, 722, 699,618.

1-Methyl-3-*n*-propylimidazolium Chloride. The product was obtained as a white solid (4.05 g, 0.0252 mol, 66.8%). Meting point: 52.0 ± 0.1 °C. Heat of fusion: 10.12 ± 0.6 kJ mol^{-1}. ^{1}H NMR ($CDCl_3$, δ/ppm relative to TMS): 0.99 (t, $CH_2CH_2CH_3$, $J = 7.3$ Hz), 1.99 (sextet, $CH_2CH_2CH_3$, $J = 7.3$ Hz), 4.14 (s, CH_3), 4.33 (t, $CH_2CH_2CH_3$, $J = 7.3$ Hz), 7.69 (s, H_4, H_5), 7.81 (s, H_4, H_5), 10.54 (s, H_2). ^{13}C NMR (δ/ppm): 10.5, 23.4, 36.3, 51.2, 122.1, 123.6, 137.4. IR (thin film on NaCl plates, ν/cm^{-1}): 3140, 3013, 2967, 2937, 2880, 1574, 1470, 1279, 1178, 733, 698, 626.

1-Methyl-3-*n*-propylimidazolium Bromide. The product was obtained as a white solid (12.58 g, 0.0613 mol, 98.3%). Melting point: 32.8 ± 1.0 °C. Heat of fusion: 14.3 ± 1.4 kJ mol^{-1}. ^{1}H NMR ($CDCl_3$, δ/ppm relative to TMS): 1.00 (t, $CH_2CH_2CH_3$, $J = 7.3$ Hz), 2.00 (sextet, $CH_2CH_2CH_3$, $J = 7.3$ Hz), 4.16 (s, CH_3), 4.36 (t, $CH_2CH_2CH_3$, $J = 7.3$ Hz), 7.73 (s, H_4, H_5), 7.83 (s, H_4, H_5), 10.23 (s, H_2). ^{13}C NMR (δ/ppm): 10.4, 23.4, 36.4, 51.1, 122.2, 123.6, 136.6. IR (thin film on NaCl plates, ν/cm^{-1}): 3140, 3008, 2936, 2879, 2850, 1574, 1470, 1276, 1179, 721, 699, 625.

1-Methyl-3-*n*-propylimidazolium Iodide. The product was obtained as a yellow liquid at room temperature (24.4 g, 0.0968 mol, 96.4%). ^{1}H NMR ($CDCl_3$, δ/ppm relative to TMS): 1.01 (t, $CH_2CH_2CH_3$, $J = 7.3$ Hz), 2.00 (sextet, $CH_2CH_2CH_3$, $J = 7.3$ Hz), 4.15 (s, CH_3), 4.35 (t, $CH_2CH_2CH_3$, $J = 7.3$ Hz), 7.68 (s, H_4, H_5), 7.70 (s, H_4, H_5), 9.91 (s, H_2). ^{13}C NMR (δ/ppm): 10.8, 23.7, 37.1, 51.5, 122.5, 123.8, 136.4. IR (neat on NaCl plates, ν/cm^{-1}): 3140, 2960, 2933, 2875, 1574, 1469, 1178, 736, 621.

1-*n*-Butyl-3-methylimidazolium Bromide. The product was obtained as an off-white solid (15.79 g, 0.0721 mol, 96.1%). Melting point: 74.3 ± 0.8 °C. Heat of fusion: 16.3 ± 1.1 kJ mol^{-1}. ^{1}H NMR ($CDCl_3$, δ/ppm relative to TMS): 0.97 (t, $CH_2CH_2CH_2CH_3$, $J = 7.3$ Hz), 1.39 (sextet, $CH_2CH_2CH_2CH_3$, $J = 7.4$ Hz), 1.93 (quint, $CH_2CH_2CH_2CH_3$ $J = 7.5$ Hz), 4.15 (s, CH_3), 4.37 (t, $CH_2CH_2CH_2CH_3$, $J = 7.5$ Hz), 7.66 (br s, H_4, H_5), 7.78 (br s, H_4, H_5), 10.28 (s, H_2). ^{13}C NMR (δ/ppm): 13.3, 19.2, 32.0, 36.5, 49.6, 122.2, 123.7, 136.8. IR (thin film on NaCl plates, ν/cm^{-1}): 3140, 3008, 2959, 2933, 2875, 1573, 1468, 1275, 1177, 721, 699, 625.

1-*n*-Butyl-3-methylimidazolium Iodide. The product was obtained as a viscous, yellow oil (129.4 g, 0.486 mol, 96.9%). ^{1}H NMR (acetone-d_6, δ/ppm relative to TMS): δ 0.90 (t, $CH_2CH_2CH_2CH_3$, $J = 7.4$ Hz), 1.35 (sextet, $CH_2CH_2CH_2CH_3$, $J = 7.5$ Hz), 1.92 (quint, $CH_2CH_2CH_2CH_3$, $J = 7.4$ Hz), 4.11 (s, CH_3), 4.45 (t, $CH_2CH_2CH_2CH_3$, $J = 7.4$ Hz), 7.97 (br s, H_4, H_5), 8.08 (br s, H_4, H_5), 9.77 (s, H_2). ^{13}C NMR (δ/ppm): 14.1, 20.1, 33.0, 37.6, 50.2, 123.5, 124.7, 138.0. IR (neat on NaCl plates, ν/cm^{-1}): 3139, 2957, 2932, 2873, 1573, 1466, 1173, 751, 618.

Quantum Mechanical Method

Calculations were performed using Gaussian 98, utilizing the 6-31G*[18] and 6-31+G*[19] basis sets. For iodine, the Huzinaga (43321/4321/41* and 433321/43321/431*) basis sets[20] were used in conjunction with the 6-31G* basis sets, augmented by diffuse functions when appropriate. All geometries were optimized via a stepping stone approach, in which the geometries at the levels HF/STO-3G, HF/3-21G, HF/6-31G*, HF/6-31+G*, MP2/6-31G*, and MP2/6-31+G* were sequentially optimized. Frequency calculations were performed after each level to verify stability, and the resulting Hessian was used in the following optimization. In the analysis of the 1-*n*-butyl-3-methylimidazolium halides, frequency calculations were omitted at the MP2 levels of theory to minimize the analysis time. Any problems in the Z-matrix coordinates would give rise to imaginary frequencies, corresponding to modes orthogonal to the spanned Z-matrix space. The Hessian was evaluated at the first geometry (opt = CalcFC) for the first level in a series to aid in geometry convergence. As the halide ions themselves possess no internal coordinates, single-point calculations at all levels were carried out.

It is unlikely that solvent effects would cause major changes in the geometry of the cation. The position of the anion relative to the cation could be affected. However, for these ion pairs, the applicability of standard dielectric models is difficult because the solvent surface of a dissociating species is rapidly changing when the distance between the cation and anion is close to the sum of the individual radii. In addition, the results depend highly on the choice of radii used. Also, the dielectric model is meant to describe the long range electrostatic polarization of the solvent, but on the molecular scale the dielectric model can hardly be expected to work. In a recent study by one of us, the Onsager model failed to account for the solvent-induced changes in the scandium-chloride distance.[25] In addition, because we are attempting to model the melting temperature (an equilibrium between two condensed phases), bulk electrostatic effects should be present in both phases and will partially cancel. We feel that the issue of how best to model bulk electrostatic effects, though important, raises deep issues that are beyond the scope of this paper. This work should be regarded as a first step up in the ab initio study of ionic liquids.

Acknowledgment. We thank the Natural Sciences and Engineering Research Council (NSERC Discovery Grants to R.D.S. and C.C.P.) and Saint Mary's University Senate Research for funding this research. We thank the Department of Astronomy and Physics, Saint Mary's University (AP-SMU), for providing access to computing facilities, in particular, to Cygnus, a 10-processor Sun server, purchased with assistance from the Canada Foundation for Innovation, Sun Microsystems, the Atlantic Canada Opportunities Agency, and SMU.

Supporting Information Available: Total energies for all structures investigated and presented in this article (Tables S1−S6) are available free of charge via the Internet at http://pubs.acs.org.

References and Notes

(1) Wasserscheid, P.; Keim W. *Angew. Chem., Int. Ed. Engl.* **2000**, *39*, 3772−3789.
(2) Huddleston, J. G.; Visser, A. E.; Reichert, W. M.; Willauer, H. D.; Broker, G. A.; Rogers, R. D. *Green Chem.* **2001**, *3*, 156−164.
(3) Welton, T. *Chem. Rev.* **1999**, *99*, 2071−2083.
(4) Earle, M. J.; Seddon, K. R. *Pure Appl. Chem.* **2000**, *72*, 1391−1398.
(5) Chiappe, C.; Capraro, D.; Conte, V., Pieraccini, D. *Org. Lett.* **2001**, *3*, 1061−1063.
(6) Stark, A.; MacLean, B.; Singer, R. D. *J. Chem. Soc., Dalton Trans.* **1999**, 63−66.
(7) Sheldon, R. *Chem. Commun.* **2001**, 2399−2407.
(8) Carmichael, A. J.; Earle, M. J.; Holbrey, J. D.; McCormac, P. B.; Seddon, K. R. *Org. Lett.* **1999**, *1*, 997−1000.
(9) Chun, S.; Dzyuba, S. V.; Bartsch, R. A. *Anal. Chem.* **2001**, *73*, 3737−3741.
(10) Fadeev, A. G.; Meagher, M. M. *Chem. Commun.* **2001**, 295−296.

(11) Schäfer, T.; Rodrigues, C. M.; Afonso, A. M.; Crespo, J. G. *Chem. Commun.* **2001**, 1622−1623.
(12) Bates, E. D.; Mayton, R. D.; Ntai, I.; Davis, J. H. *J. Am. Chem. Soc. Commun.* **2002**, *124*, 926−927.
(13) Holbrey, J. D.; Seddon, K. R. *Clean Products Processes* **1999**, *1*, 223−236.
(14) Shah, J. K.; Brennecke, J. F.; Maginn, E. J. *Green Chem.* **2002**, *4*, 112−118.
(15) Katritzky, A. R.; Lomaka, A.; Petrukhin, R.; Jain, R.; Karelson, M.; Visser, A. E.; Rogers, R. D. *J. Chem. Inf. Comput. Sci.* **2002**, *42*, 71−74.
(16) Katritzky, A. R.; Jain, R.; Lomaka, A.; Petrukhin, R.; Karelson, M.; Visser, A. E.; Rogers, R. D. *J. Chem. Inf. Comput. Sci.* **2002**, *42*, 225−231.
(17) Sitze, M. S.; Schreiter, E. R.; Patterson, E. V.; Freeman, R. G. *Inorg. Chem.* **2001**, *40*, 2298−2304.
(18) Hehre, W. J.; Ditchfield, R.; Pople, J. A. *J. Chem. Phys.* **1972**, *56*, 2257−2261. Hariharan, P. C.; Pople, J. A. *Theor. Chim. Acta* **1973**, *28*, 213−222. Francl, M. M.; Pietro, W. J.; Hehre, W. J.; Binkley, J. S.; Gordon, M. S.; Defrees, D. J.; Pople, J. A. *J. Chem. Phys.* **1982**, *77*, 3654−3665. Binning, R. C., Jr.; Curtiss, L. A. *J. Comput. Chem.* **1990**, *11*, 1206.
(19) Clark, T.; Chandrasekhar, J.; Spitznagel, G. W.; v. R. Schleyer, P. *J. Comput. Chem.* **1983**, *4*, 294−301. Frisch, M. J.; Pople, J. A.; Binkley, J. S. *J. Chem. Phys.* **1984**, *80*, 3265−3269.
(20) Huzinaga, S.; Andzelm, J.; Klobutowski, M.; Radio-Andzelm, E.; Sakei, Y.; Tatewaki, H. *Gaussian Basis Sets for Molecular Calculations*; Elsevier: Amsterdam, 1984.
(21) Dymek, C. J.; Grossie, D. A.; Fratini, A. V.; Adams, W. W. *J. Mol. Struct.* **1989**, *213*, 25−34.
(22) Elaiwi, A.; Hitchcock, P. B.; Seddon, K. R.; Srinivasan, N.; Tan, Y.-M.; Welton, T.; Zora, J. A. *J. Chem. Soc., Dalton Tran.* **1995**, 3467−3472.
(23) Abdul-Sada, A. K.; Greenway, A. M.; Hitchcock, P. B.; Mohammed, T. J.; Seddon, K. R.; Zora, J. A. *J. Chem. Soc., Chem. Commun.* **1986**, 1753−1754.
(24) Loudon, G. M. *Organic Chemistry*, 3rd ed.; The Benjamin/Cummings Publishing Co., Inc.: CA, 1995; pp 70−71.
(25) Pye, C. C.; Corbeil, C. R. *Can. J. Chem.* **2002**, *80*, 1331−1342.